Proceedings of the 28th IEEE
EMBS Annual International Conference
New York City, USA, Aug 30-Sept 3, 2006

SaB05.3

Novel Measurement Method for Magnetic Particles

J. Mäkiranta, J. Verho, J. Lekkala and N. Matintupa*
Institute of Measurement and Information Technology, Tampere University of Technology, Tampere, Finland
*Department of Biochemistry, University of Jyväskylä, Jyväskylä, Finland

Abstract — **This paper represents a novel magnetic nanoparticle measurement method for applications in clinical diagnostics. Planar microcoils and impedance bridge measurement are used to measure the amount of the particles. Macro size coils made on PCB are used to test and verify the measurement method and measurement electronics. Experimental tests and simulative results will be used for a future microscale sensing system.**

Index Terms—**magnetic particle, planar micro coil, impedance bridge, permeability**

I. Introduction

THE need for point-of-care (POC) testing made at home or doctor's office has increased rapidly during the last years. Aging of population, threat of pandemic and need for doping tests, for example, create new demands for clinical diagnostics. Expensive and time-consuming laboratory tests can be reduced without losing reliability of a diagnosis. The POC tests make the diagnosis faster, simpler, and more affordable. [1]

These tests use sophisticated immunodiagnostic assays based on specific binding and immunocomplex formation between two molecules, antibody and antigen (also known as analyte). The most common principle utilizes a special labeling technique. Instead of measuring analyte molecules directly special particles used as labels are detected. The number of label particles is proportional to the amount of target molecules. The use of label typically increases sensitivity and decreases detection limit. [2]

Magnetic nanoparticles (MNP) are small ferrite oxides (such as magnetite, Fe_3O_4) typically ranging from few nanometers to few micrometers in diameter. Magnetic nanoparticle can be a single bead or bead cluster closed in a polymer matrix.

This work was supported by the Finnish Funding Agency for Technology and Innovation (TEKES) in Finnwell research program.

J. J. Mäkiranta is with the Institute of Measurement and Information Technology in Tampere University of Technology, Tampere, Finland (phone: +358-3-31153579; fax:+358-3-31152171; e-mail: jarkko.makiranta@tut.fi).

J. Verho is with the Institute of Measurement and Information Technology in Tampere University of Technology, Tampere, Finland (e-mail: jarmo.verho@tut.fi).

J. O. Lekkala is with the Institute of Measurement and Information Technology in Tampere University of Technology, Tampere, Finland (e-mail: jukka.lekkala@tut.fi).

N. Matintupa is with the Department of Biochemistry in University of Jyväskylä, Jyväskylä, Finland (e-mail: nkmatint@cc.jyu.fi).

The magnetic nanoparticles can be used as a magnetic label in immunodiagnostic. The measurement of the MNP label is substantially safer compared to radioactive labels and more affordable when compared to optical measurement methods using fluorescent labels. The magnetic labels have also other advantages; because they can be manipulated with an external field. This allows etc. sample separation, purification and transportation in POC chip. [3]

II. Theory

A. Sensor Design and Bridge Layout

A set of identical planar microcoils aligned symmetrically in an impedance bridge is the base of the sensor system. The magnetic nanoparticles are placed on the sensing coil (coil A in Fig 1.). MNPs change the inductance of the coil due to the change in relative permeability. The change in inductance unbalances (Eq. 1) the bridge at high frequency (1 to 100 MHz) because of change of inductive reactance.

$$\Delta U = \frac{U}{4Z}\Delta Z, \qquad (1)$$

where U is voltage, Z is impedance and ΔU and ΔZ are voltage change and impedance change respectively.

An experimental macroscale coil bridge was designed using numerical modeling tools and fabricated on PCB (Printed Circuit Board). The designed macroscale sensor bridge will be later used in verification of a future microscale POC compatible sensor bridge.

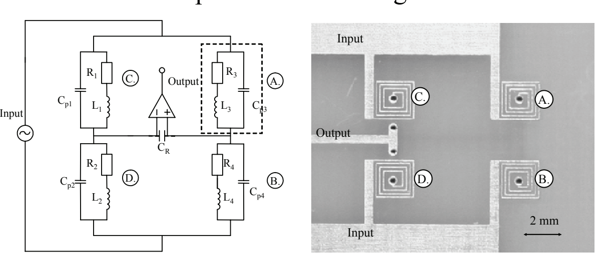

Fig. 1. Equivalent circuit of impedance bridge (left) and layout of the sensor (right). Sensing coil (A), reference coil (B) and compensation coils (C and B) are marked.

Studied macroscale structure contains four identical rectangular spiral coils with 4 turns in each. The coils are made of copper on FR-4 substrate. The copper layer is 36 µm thick and is coated with gold to prevent oxidation. The designed width and spacing of coil wires are 75 µm and 125 µm, respectively. The cross-section of the coil is 2.1 mm.

B. Analytical Model for the Coil

The sensor layout has been designed (for experimental research) and further improved and optimized using numerical modeling methods and analytical solution for the coil. The dimensions (spacing, width) and other parameters (frequency, driving voltage, and size of the MNP sample area) were studied and selected using this solution.

A sensitivity of the sensing system is strongly dependent on the inductance (inductive reactance) of the coil. Analytical expression in Eq. 2 is used for inductance. [4].

$$L = \frac{\mu_0 N^2 d_{avg} c1}{2} (\ln \frac{c2}{\rho} + c3\rho + c4\rho^2), \quad (2)$$

$$d_{avg} = 0.5(d_{out} + d_{in}), \quad (3)$$

$$\rho = \frac{d_{out} - d_{in}}{d_{out} + d_{din}}, \quad (4)$$

where μ_0 is permeability of the vacuum, N is number of turns, d_{out}, d_{in} and d_{avg} are outer -, inner - and average diameters respectively. ρ is fill ratio and c_1 - c_4 are shape depending constants (defined in Table 2.1). [4].

Table 2.1

Parameters for different shape of spiral coils [4]

Shape	**c1**	**c2**	**c3**	**c4**
Square	1.27	2.07	0.18	0.13
Hexagon	1.09	2.23	0.00	0.17
Octagon	1.07	2.29	0.00	0.19
Circle	1.00	2.46	0.00	0.20

Commonly known expression (Eq. 5) of the resistance is:

$$R_s = \frac{\rho l}{A} = \frac{\rho l}{wt}, \quad (5)$$

where ρ is the resistivity of the material (for copper $1.678 \cdot 10^{-8}$ Ωm), l is the length of the current sheet (formula below), w is the width of the wire and t is the thickness of the wire. For high frequency skin depth must be taken into account. That is why t should be given as effective thickness (Eq. 7).

The length of the current sheets can be approximated using Eq. 6 [4].

$$l = N d_{avg} N_{sides} \tan(\frac{\pi}{N_{sides}}), \quad (6)$$

where N is the number of turns ($N = 4$), N_{sides} is the number of sides (for square 4) [4].

The effective thickness of the wire can be approximated with

$$t_{eff} = \int_0^t e^{-\frac{z}{\delta}} dz = \sqrt{\frac{1}{\pi f \mu \sigma}} (1 - e^{-\frac{t}{\sqrt{\frac{1}{\pi f \mu \sigma}}}}), \quad (7)$$

where f is the frequency, σ is the electric conductivity ($1 / \rho$) and μ is permeability (in this case just μ_0). [4]

Using presented expression the impedance can be calculated as

$$Z = \sqrt{R^2 + (X_L^2 - X_C^2)}, \quad (8)$$

where R is the resistance, X_L inductive reactance and X_c capacitive reactance. In this case (relative small dimensions) we can approximate that $X_c \rightarrow 0$.

Calculated and measured coil parameters at 7 MHz frequency can be found in Table 2.2. Coil parameters were measured with an Agilent 4396B impedance analyzer and a probe station. Measured values differ from analytical ones because of the contact sheets needed for the measuring.

Table 2.2

Coil parameters

	L [nH]	R [mΩ]	Z [Ω]
Analytical	28,9	273	1,30
Measured	29,8	280	1,34

C. Numerical Model for the Coil

Numerical methods like FEM (Finite Element Method) were used for describing the interactions between the sensing coil and magnetic nanoparticles (Fig. 2.). Model was built using 2D axial symmetry. Maxwell's equations were solved using FEM and the inductance of the coil was integrated from the solution.

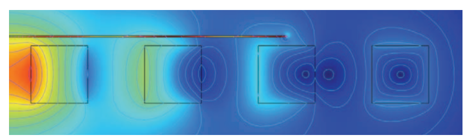

Fig.2. Numerical 2D axial symmetric simulation. Interaction between sensing coil (4 squares) and magnetic nanoparticles (rectangle above coils).

The change of relative permeability due the MNPs was studied with FEM but also with first preliminary measurements using the impedance analyzer and the probe station. Appropriate objective for detection limit was set to μ_r~1.00001. This is beyond the sensitivity of the impedance analyzer. Need for more precise measurement device was obvious.

Using calculated parameters from Table 2.2 for the coil, set value for the permeability (μ_r~1.00001) and Eq.1 an approximate value for the output was solved; ΔU~0.3 µV. This approximation was the base for the measurement electronics.

III. Measurement Electronics

There were two main design objectives for the hardware, namely a wide operating frequency range (1...30MHz) and a high S/N ratio. Also, sine wave excitation for the detector coils and an ability to measure phase shifts were considered as desirable features.

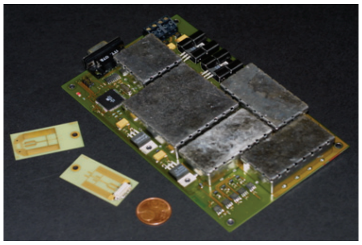

Fig. 3. Measurement device with impedance bridges.

As it was known that the magnetic particles had only a very small effect on the measurement coil inductance ($\mu_r \sim$ 1.00001) and as there was a need to compensate environmental influences on the measurement coils, the Wheatstone bridge was a quite obvious choice.

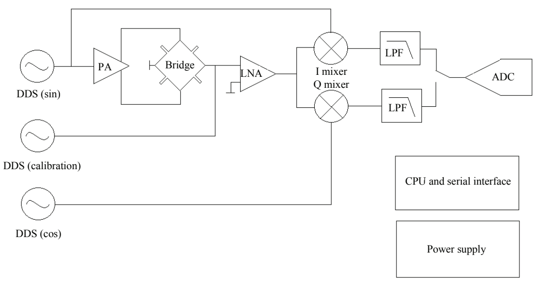

Fig. 4. Block diagram of the measurement device.

DDS (Direct Digital Synthesis) oscillators were used to generate the required adjustable sine excitation signal. To maximize the noise immunity, the bridge drive and measurement were floated using transformers. As the output signal from the bridge was rather weak, a high gain, low noise, wideband amplifier was used. The first stages of the amplifier were implemented using low noise transistors and the rest of the amplifier with CFB (Current Feedback) operational amplifiers. The total gain of the amplifier block was nominally 30000.

A quadrature detection was used to reduce low frequency noise, 50 Hz pick-ups signal, and to be able to measure phase differences. Instead of the usual Gilbert cell mixers (commonly used in RF applications), wideband analog multipliers were used to reduce spurious responses. Required cosine input for the Q (quadrature) mixer was generated by using another DDS oscillator. Multiplier outputs were then filtered, amplified and fed to a 16b ADC.

In spite of symmetry of the measurement coil bridge layout and good PCB house, there were still significant differences between the coils of the bridge. To counteract that problem, the third DDS oscillator was added. Its purpose was to supply controlled amplitude, controlled phase balancing signal to the bridge output so that the bridge output was forced to zero when there were no particles.

To reduce noise level and to prevent crosstalk between modules, extensive shielding and power supply filtering was used. Also, every major module had its own regulator.

Instrument operation was controlled by a small 8-bit CPU (Central Processing Unit). It connected to a PC via RS-232, offering a simple command interpreter interface to the user.

IV. Methodology

A. Sample preparation

Magnetic nanoparticles used for the measurements were made by Estapor® Microspheres [5]. Diameter of the MNPs varies from 300 nm to 500 nm. They were formed from smaller magnetite Fe_3O_4 particles about 10 nm in diameter.

Two kinds of samples were used: MNPs in a porous strip for testing of linearity and MNPs on a microscope slide for testing of sensitivity.

Constant areas of magnetic particles (1 mm x 1 mm) with different dilution ratios (1/4, 1/16, 1/64 and 1/256) were absorbed (absorbing depth 100 µm) in porous strips (Fig. 5 2.). The dilution ratio defines how much base solution (base solution = magnetic particles in saline solution) has been diluted. Accurate amount of magnetic particles per dilution ratio was not known.

Porous strips were attached on a plastic rectangle (Fig. 5 1.) for easier handling. Porous sheet and magnetic particles (Fig. 5 3.) were covered with 60 µm thick insulation layer of Scotch tape (Fig. 5 4.).

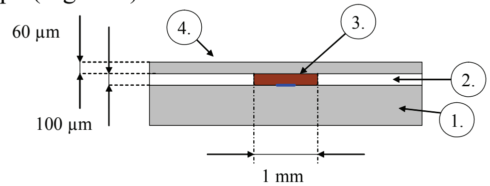

Fig. 5. Sample rectangle. Plastic rectangle (1.), porous strip (2.), magnetic particles (3.) and insulating tape (4.).

Dilution ratios were simple but imperfect definition for amount of the particles. Need for absolute estimate particle number was obvious. Constant density and area (A_{sample} = 1 mm x 1 mm) of magnetic particles were injected on the microscope slide. Density profile was imaged using an optical microscope with 50X magnification. After image processing with Matlab® (removing noise, distortion and holes) 22 % coverage (η) was found. Assuming that particles form monolayers and that the density profile is constant, total number of 1.75 million particles (size of single MNP averaged to 400 nm) was estimated for the area of 1 mm x 1 mm (Eq. 9).

$$N = \frac{A_{sample}}{A_{MNP}} \eta \qquad (9)$$

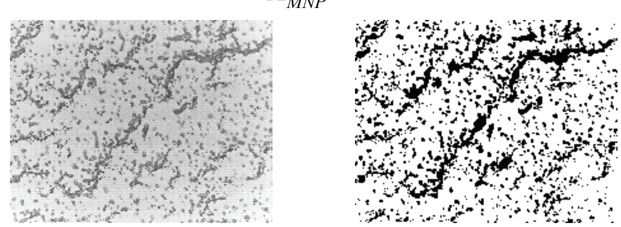

Fig. 6. Calibration sample with 22 % coverage of magnetic particles. Left picture presents original TIF – image. Right picture has been processed with Matlab®.

B. Measurement setup

The sample (different ratios of magnetic nanoparticles and microscope slide with constant particle density) was aligned near to the surface of the sensor coil with XYZ – stage. Particle free reference zone of the sample was simultaneously aligned on the coil B. This was made to eliminate the error signal caused by the porous strip.

First the sample was aligned on coil A and bridge was calibrated and measured at 7 MHz. After this the sample was pulled up and the difference was measured. This procedure was repeated totally 20 times (10 times for coil A and 10 times for coil B) for each (5) sample.

V. Results

Output signal of the impedance bridge is presented in Table 5.1. The results have been separated for different samples (4, 16, 64, 256 and cal) and measurements (A is for left coil, B is for right). Results are in μV. Standard deviation for repeatability (each measurement was repeated 5 times) is presented.

Table 5.1
Output signal of the impedance bridge.

	A1	A2	B1	B2
U_4	**113,90**	**114,55**	**93,46**	**97,59**
σU_4	0,65	0,69	0,96	1,56
U_{16}	**28,55**	**25,97**	**27,44**	**27,24**
σU_{16}	0,41	2,51	1,21	1,00
U_{64}	**13,30**	**11,45**	**12,30**	**10,99**
σU_{64}	3,56	2,07	3,80	4,30
U_{256}	**5,96**	**5,02**	**6,64**	**7,26**
σU_{256}	1,95	1,70	0,79	1,66
U_{cal}	**13,81**	**14,49**	**15,86**	**14,81**
σU_{cal}	0,74	0,63	0,87	0,49

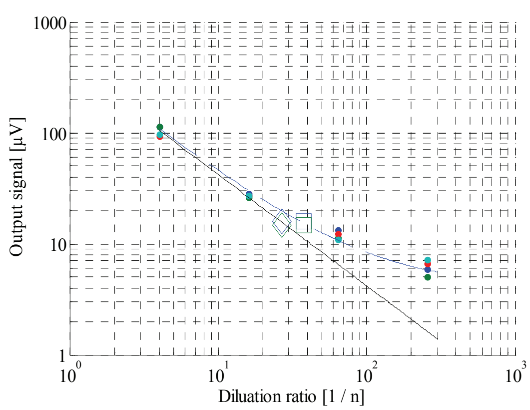

Fig. 7. Output signal of the sensor bridge with different samples. Dashed blue line expresses the trend of the measurement. Solid black line expresses the calculated trend based on first two dilution ratios Note the logarithmic axes. Results from the calibration sample are added on both curves.

Measurement data was analyzed with Matlab®. Drifting was removed and noise was averaged. Results with higher dilution ratios suffer from cumulative inaccuracies in sample preparation. That can be seen as drift from trend line calculated from first two dilution ratios (Fig. 7).

VI. Discussion

Using a calibration sample of total number of 1.75 millions of particles the output signal of the bridge is 14.7 μV (average from Table 3) with S/N ratio of about 29 (Amplitude of the noise was about 500 nV (rms)). This sets the detection limit of the macro scale sensing system to 60 000 particles (with the area of 1 mm x 1 mm and particle about 400 nm in diameter).

Scaling of the results down to microscale (coil diameter about 200 – 300 μm and sample area size 100 – 300 μm) it could be possible to measure number of particles $10^3 – 10^4$. Most likely sensitivity would suffer for small inductance and increase of resistance due to thinner conductors.

VII. Conclusions

Novel measurement method of magnetic particles has been studied with numerical simulations, analytical approximations and experimental measurements. Measurement results have been calibrated using the constant density MNP sample. Planar microcoils and distortion immune bridge measurement allow sensitivity of 8.4 pV / MNP.

VIII. Acknowledgment

The authors would like to express their sincere thanks to M. Laitinen from University of Jyväskylä for samples and to the Finnish Funding Agency for Technology and Innovation for funding the project (Finwell, 820/31/05).

References

[1] The British In Vitro Diagnostics Association, http://www.bivda.co.uk/, referred 28.4.2006

[2] B. R. Egging, Chemical Sensors and Biosensors, Wiley, p. 298, 2002

[3] J.J. Mäkiranta, J. O. Lekkala "Modeling and Simulation of Magnetic Nanoparticle Sensor," IEEE Engineering in Medicine and Biology Society, 01-04 Sept. 2005 Page(s):1256 – 1259.

[4] S. S. Mohan, The design, modeling, and optimization of on-chip inductor and transformer circuits, Ph.D. dissertation Stanford, CA: Stanford Univ., Dec. 1999.

[5] Estapor® Microspheres, http://www.estapor.com/, referred 10.7.2006.